Today's outline - October 14, 2024

Today's outline - October 14, 2024

- Ewald sphere

Today's outline - October 14, 2024

- Ewald sphere
- XRayView demonstration

Today's outline - October 14, 2024

- Ewald sphere
- XRayView demonstration
- Crystal truncation rods

Today's outline - October 14, 2024

- Ewald sphere
- XRayView demonstration
- Crystal truncation rods
- Diffuse Scattering

Today's outline - October 14, 2024

- Ewald sphere
- XRayView demonstration
- Crystal truncation rods
- Diffuse Scattering
- Modulated structures

Today's outline - October 14, 2024

- Ewald sphere
- XRayView demonstration
- Crystal truncation rods
- Diffuse Scattering
- Modulated structures
- Lattice vibrations

Today's outline - October 14, 2024

- Ewald sphere
- XRayView demonstration
- Crystal truncation rods
- Diffuse Scattering
- Modulated structures
- Lattice vibrations

Reading Assignment: Chapter 5.5-5.6

Today's outline - October 14, 2024

- Ewald sphere
- XRayView demonstration
- Crystal truncation rods
- Diffuse Scattering
- Modulated structures
- Lattice vibrations

Reading Assignment: Chapter 5.5-5.6

Homework Assignment #04:
Chapter 4: 2,4,6,7,10
due Friday, October 18, 2024

Today's outline - October 14, 2024

- Ewald sphere
- XRayView demonstration
- Crystal truncation rods
- Diffuse Scattering
- Modulated structures
- Lattice vibrations

Reading Assignment: Chapter 5.5-5.6

Homework Assignment #04:
Chapter 4: 2,4,6,7,10
due Friday, October 18, 2024

Homework Assignment #05:
Chapter 5: 1,3,7,9,10
due Monday, October 28, 2024

The Ewald sphere

The Ewald sphere is a construct which permits the enumeration of reflections which fulfill the Laue diffraction condition.

The Ewald sphere

The Ewald sphere is a construct which permits the enumeration of reflections which fulfill the Laue diffraction condition.

The sphere radius is set by the length of the $\vec{k}$ and $\vec{k}'$ vectors which characterize the incident and scattered (where the detector is placed) x-rays and $\Delta\vec{k}$ being the bandwidth of the incident x-rays

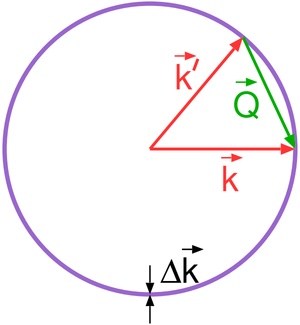

The Ewald sphere

The Ewald sphere is a construct which permits the enumeration of reflections which fulfill the Laue diffraction condition.

The sphere radius is set by the length of the $\vec{k}$ and $\vec{k}'$ vectors which characterize the incident and scattered (where the detector is placed) x-rays and $\Delta\vec{k}$ being the bandwidth of the incident x-rays

As the detector moves, $\vec{k}'$ rotates but the Ewald sphere remains constant.

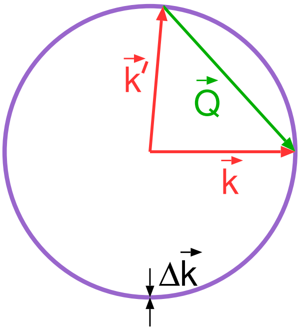

The Ewald sphere

The Ewald sphere is a construct which permits the enumeration of reflections which fulfill the Laue diffraction condition.

The sphere radius is set by the length of the $\vec{k}$ and $\vec{k}'$ vectors which characterize the incident and scattered (where the detector is placed) x-rays and $\Delta\vec{k}$ being the bandwidth of the incident x-rays

As the detector moves, $\vec{k}'$ rotates but the Ewald sphere remains constant.

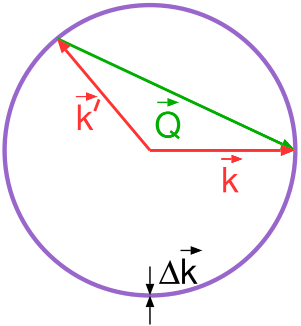

The Ewald sphere

The Ewald sphere is a construct which permits the enumeration of reflections which fulfill the Laue diffraction condition.

The sphere radius is set by the length of the $\vec{k}$ and $\vec{k}'$ vectors which characterize the incident and scattered (where the detector is placed) x-rays and $\Delta\vec{k}$ being the bandwidth of the incident x-rays

As the detector moves, $\vec{k}'$ rotates but the Ewald sphere remains constant.

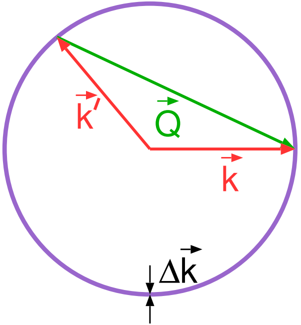

The xrayview program can be used to gain a more intuitive understanding of the Ewald sphere.

The Ewald sphere

The Ewald sphere is a construct which permits the enumeration of reflections which fulfill the Laue diffraction condition.

The sphere radius is set by the length of the $\vec{k}$ and $\vec{k}'$ vectors which characterize the incident and scattered (where the detector is placed) x-rays and $\Delta\vec{k}$ being the bandwidth of the incident x-rays

As the detector moves, $\vec{k}'$ rotates but the Ewald sphere remains constant.

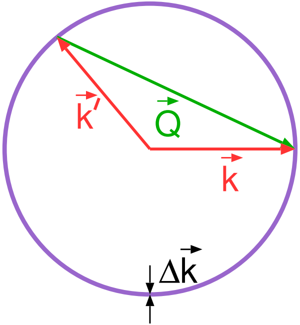

The xrayview program can be used to gain a more intuitive understanding of the Ewald sphere.

http://www.phillipslab.org/software

Ewald sphere & the reciprocal lattice

The reciprocal lattice is defined by the unit vectors $\vec{a}_1^*$ and $\vec{a}_2^*$.

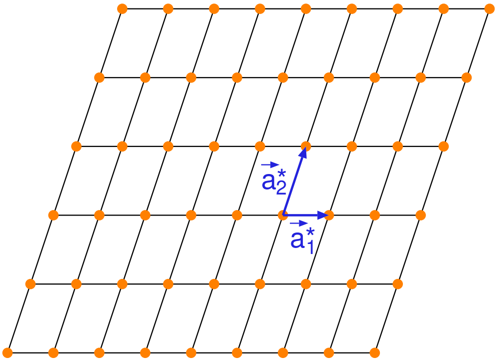

Ewald sphere & the reciprocal lattice

The reciprocal lattice is defined by the unit vectors $\vec{a}_1^*$ and $\vec{a}_2^*$.

The key parameter is the relative orientation of the incident wave vector $\vec{k}$

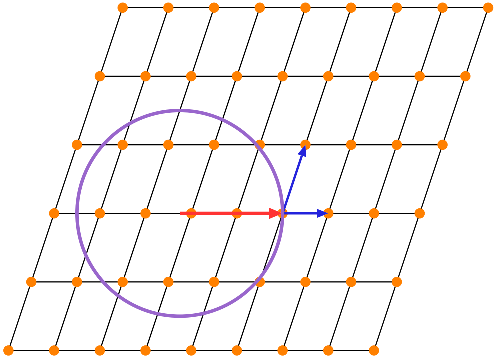

Ewald sphere & the reciprocal lattice

The reciprocal lattice is defined by the unit vectors $\vec{a}_1^*$ and $\vec{a}_2^*$.

The key parameter is the relative orientation of the incident wave vector $\vec{k}$

As the crystal is rotated with respect to the incident beam, the reciprocal lattice also rotates

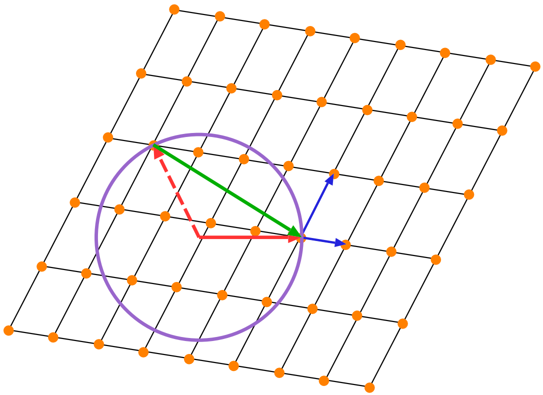

Ewald sphere & the reciprocal lattice

The reciprocal lattice is defined by the unit vectors $\vec{a}_1^*$ and $\vec{a}_2^*$.

The key parameter is the relative orientation of the incident wave vector $\vec{k}$

As the crystal is rotated with respect to the incident beam, the reciprocal lattice also rotates

When the Ewald sphere intersects a reciprocal lattice point there will be a diffraction peak in the direction of the scattered x-rays.

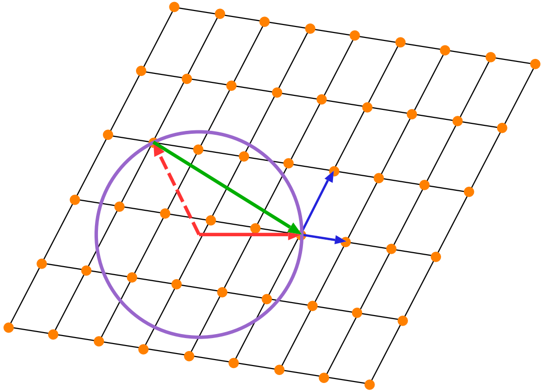

Ewald sphere & the reciprocal lattice

The reciprocal lattice is defined by the unit vectors $\vec{a}_1^*$ and $\vec{a}_2^*$.

The key parameter is the relative orientation of the incident wave vector $\vec{k}$

As the crystal is rotated with respect to the incident beam, the reciprocal lattice also rotates

When the Ewald sphere intersects a reciprocal lattice point there will be a diffraction peak in the direction of the scattered x-rays. The diffraction vector, $\vec{Q}$, is thus a reciprocal lattice vector

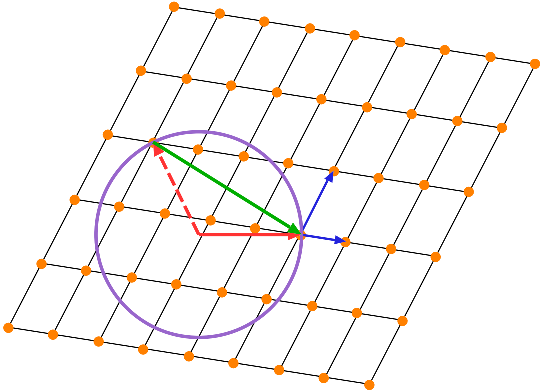

Ewald sphere & the reciprocal lattice

The reciprocal lattice is defined by the unit vectors $\vec{a}_1^*$ and $\vec{a}_2^*$.

The key parameter is the relative orientation of the incident wave vector $\vec{k}$

As the crystal is rotated with respect to the incident beam, the reciprocal lattice also rotates

When the Ewald sphere intersects a reciprocal lattice point there will be a diffraction peak in the direction of the scattered x-rays. The diffraction vector, $\vec{Q}$, is thus a reciprocal lattice vector

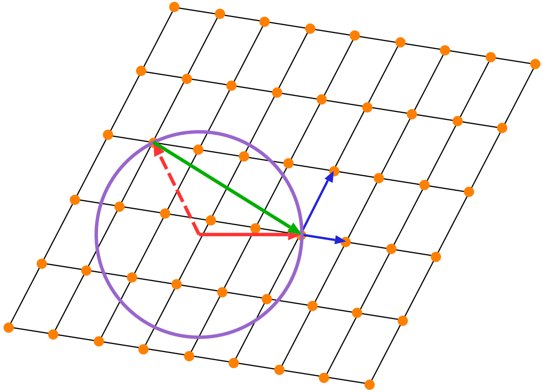

$$\vec{G}_{hlk} = h\vec{a}_1^* + k\vec{a}_2^*$$

Ewald construction

It is often more convenient to visualize the Ewald sphere by keeping the reciprocal lattice fixed and "rotating" the incident beam to visualize the scattering geometry.

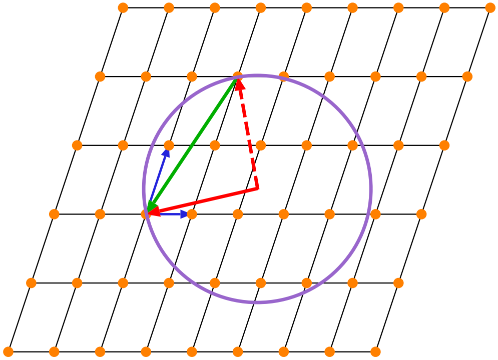

Ewald construction

It is often more convenient to visualize the Ewald sphere by keeping the reciprocal lattice fixed and "rotating" the incident beam to visualize the scattering geometry.

In directions of $\vec{k}'$ (detector position) where there is no reciprocal lattice point, there can be no diffraction peak.

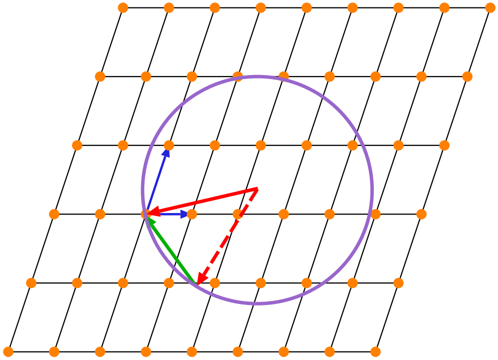

Ewald construction

It is often more convenient to visualize the Ewald sphere by keeping the reciprocal lattice fixed and "rotating" the incident beam to visualize the scattering geometry.

In directions of $\vec{k}'$ (detector position) where there is no reciprocal lattice point, there can be no diffraction peak.

If the crystal is rotated slightly with respect to the incident beam, $\vec{k}$, there may be no Bragg reflections possible at all.

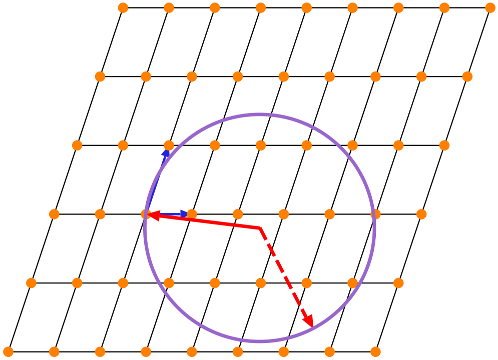

Polychromatic radiation

If $\Delta\vec{k}$ is large enough, there may be more than one reflection lying on the Ewald sphere.

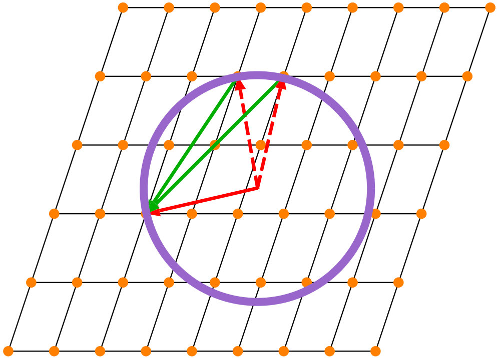

Polychromatic radiation

If $\Delta\vec{k}$ is large enough, there may be more than one reflection lying on the Ewald sphere.

With an area detector, there may then be multiple reflections appearing for a particular orientation (very common with protein crystals where the unit cell is very large).

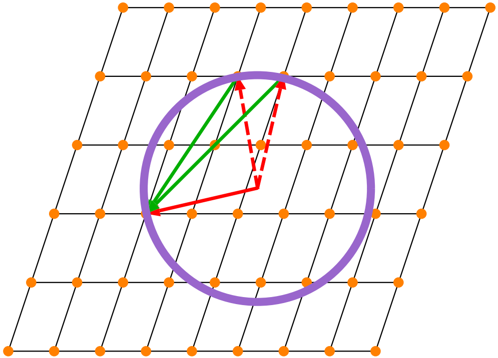

Polychromatic radiation

If $\Delta\vec{k}$ is large enough, there may be more than one reflection lying on the Ewald sphere.

With an area detector, there may then be multiple reflections appearing for a particular orientation (very common with protein crystals where the unit cell is very large).

In protein crystallography, the area detector is in a fixed location with respect to the incident beam and the crystal is rotated on a spindle so that as Laue conditions are met, spots are produced on the detector at the diffraction angle

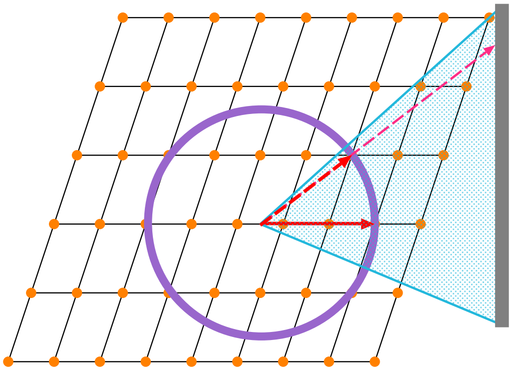

Multiple scattering

If more than one reciprocal lattice point is on the Ewald sphere, scattering can occur internal to the crystal.

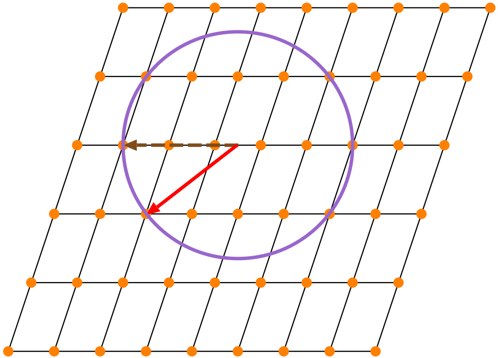

Multiple scattering

If more than one reciprocal lattice point is on the Ewald sphere, scattering can occur internal to the crystal.

The xrays are first scattered along $\vec{k}_{int}$

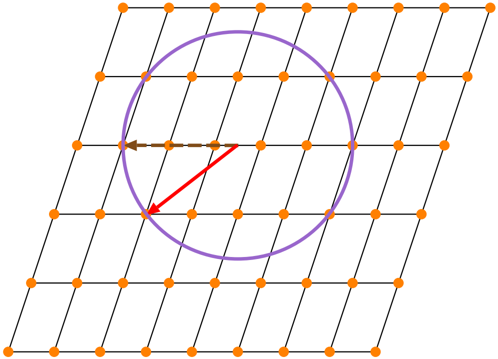

Multiple scattering

If more than one reciprocal lattice point is on the Ewald sphere, scattering can occur internal to the crystal.

The xrays are first scattered along $\vec{k}_{int}$ then along the reciprocal lattice vector which connects the two points on the Ewald sphere, $\vec{G}$

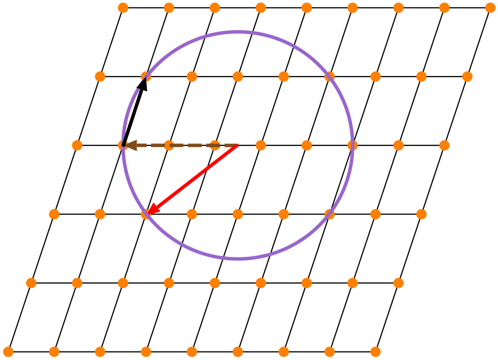

Multiple scattering

If more than one reciprocal lattice point is on the Ewald sphere, scattering can occur internal to the crystal.

The xrays are first scattered along $\vec{k}_{int}$ then along the reciprocal lattice vector which connects the two points on the Ewald sphere, $\vec{G}$ and to the detector at $\vec{k}'$.

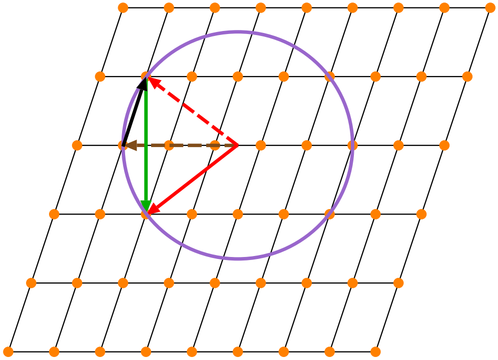

Multiple scattering

If more than one reciprocal lattice point is on the Ewald sphere, scattering can occur internal to the crystal.

The xrays are first scattered along $\vec{k}_{int}$ then along the reciprocal lattice vector which connects the two points on the Ewald sphere, $\vec{G}$ and to the detector at $\vec{k}'$.

This is the cause of monochromator glitches which sometimes remove intensity but can also add intensity to the reflection the detector is set to measure.

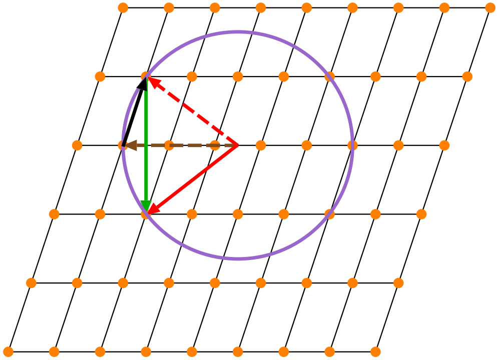

Laue diffraction

The Laue diffraction technique uses a wide range of radiation from $\vec{k}_{min}$ to $\vec{k}_{max}$

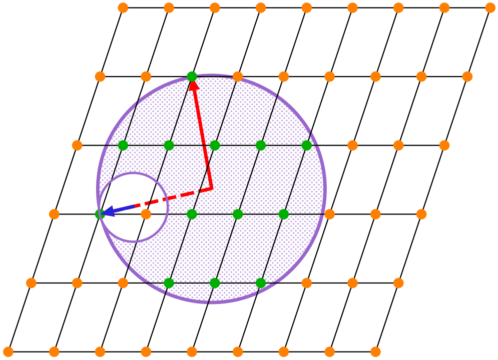

Laue diffraction

The Laue diffraction technique uses a wide range of radiation from $\vec{k}_{min}$ to $\vec{k}_{max}$

These define two Ewald spheres and a volume between them such that any reciprocal lattice point which lies in the volume will meet the Laue condition for reflection.

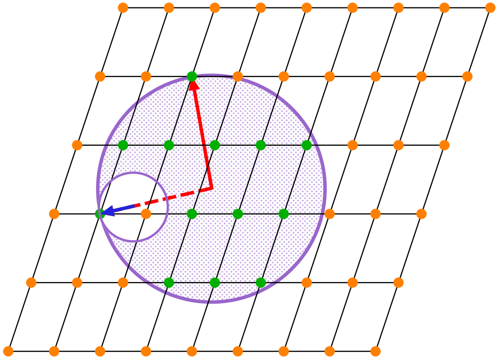

Laue diffraction

The Laue diffraction technique uses a wide range of radiation from $\vec{k}_{min}$ to $\vec{k}_{max}$

These define two Ewald spheres and a volume between them such that any reciprocal lattice point which lies in the volume will meet the Laue condition for reflection.

This technique is useful for taking data on crystals which are changing or may degrade in the beam with a single shot of x-rays on a 2D detector.

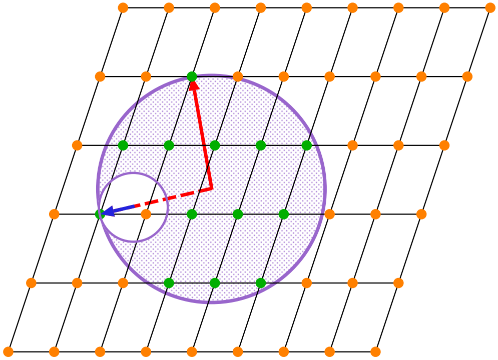

Diffraction resources

XRayView

http://www.phillipslab.org/downloads

Diffraction resources

XRayView

http://www.phillipslab.org/downloads

Bilbao Crystallography Server

http://www.cryst.ehu.es/

Diffraction resources

XRayView

http://www.phillipslab.org/downloads

Bilbao Crystallography Server

http://www.cryst.ehu.es/

Hypertext Book of Space Groups

http://img.chem.ucl.ac.uk/sgp/mainmenu.htm

Diffraction resources

XRayView

http://www.phillipslab.org/downloads

Bilbao Crystallography Server

http://www.cryst.ehu.es/

Hypertext Book of Space Groups

http://img.chem.ucl.ac.uk/sgp/mainmenu.htm

GSAS-II

https://subversion.xray.aps.anl.gov/trac/pyGSAS

XRayView demonstration

Exercise 1 - Ewald sphere

Exercise 4 - Wavelength

Exercise 8 - Laue diffraction

Exercise 9 - Serial crystallography

$P23$ $\quad$ $P\,2\,3$ $\quad$ 23 $\quad$ No. 195

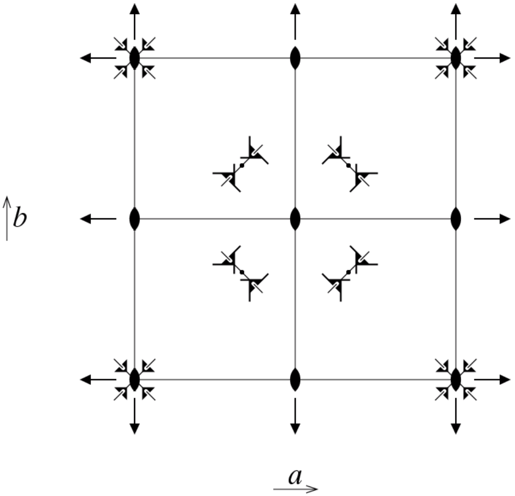

1 x, y, z
2 $x, \bar{y}, \bar{z}$
3 $\bar{x}, y, \bar{z}$
4 $\bar{x}, \bar{y}, z$
5 z, x, y
6 $\bar{z}, \bar{x}, y$
7 $z, \bar{x}, \bar{y}$
8 $\bar{z}, x, \bar{y}$
9 y, z, x
10 $\bar{y}, z, \bar{x}$
11 $\bar{y}, \bar{z}, x$
12 $y, \bar{z}, \bar{x}$

$Fd\bar{3}m$ $\quad$ $F\,4_1/d\,\bar{3}\,2/m$ $\quad$ $m\bar{3}m$ $\quad$ No. 227

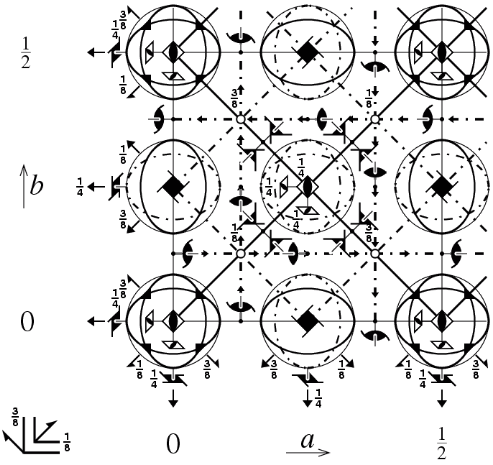

1	x, y, z	25	$\frac14-x, \frac14-y, \frac14-z$
2	$x, \bar{y}, \bar{z}$	26	$\frac14-x, \frac14+y, \frac14+z$
3	$\bar{x}, y, \bar{z}$	27	$\frac14+x, \frac14-y, \frac14+z$
4	$\bar{x}, \bar{y}, z$	28	$\frac14+x, \frac14+y, \frac14-z$
5	z, x, y	29	$\frac14-z, \frac14-x, \frac14-y$
6	$\bar{z}, \bar{x}, y$	30	$\frac14+z, \frac14+x, \frac14-y$
7	$z, \bar{x}, \bar{y}$	31	$\frac14-z, \frac14+x, \frac14+y$
8	$\bar{z}, x, \bar{y}$	32	$\frac14+z, \frac14-x, \frac14+y$
9	y, z, x	33	$\frac14-y, \frac14-z, \frac14-x$
10	$\bar{y}, z, \bar{x}$	34	$\frac14+y, \frac14-z, \frac14+x$
11	$\bar{y}, \bar{z}, x$	35	$\frac14+y, \frac14+z, \frac14-x$
12	$y, \bar{z}, \bar{x}$	36	$\frac14-y, \frac14+z, \frac14+x$
13	$\frac14+x, \frac14-z, \frac14+y$	37	$\bar{x}, z, \bar{y}$
14	$\frac14+x, \frac14+z, \frac14-y$	38	$\bar{x}, \bar{z}, y$
15	$\frac14-x, \frac14-z, \frac14-y$	39	x, z, y
16	$\frac14-x, \frac14+z, \frac14+y$	40	$x, \bar{z}, \bar{y}$
17	$\frac14+z, \frac14+y, \frac14-x$	41	$\bar{z}, \bar{y}, x$
18	$\frac14-z, \frac14+y, \frac14+x$	42	$z, \bar{y}, \bar{x}$
19	$\frac14-z, \frac14-y, \frac14-x$	43	z, y, x
20	$\frac14+z, \frac14-y, \frac14+x$	44	$\bar{z}, y, \bar{x}$
21	$\frac14-y, \frac14+x, \frac14+z$	45	$y, \bar{x}, \bar{z}$
22	$\frac14+y, \frac14-x, \frac14+z$	46	$\bar{y}, x, \bar{z}$
23	$\frac14-y, \frac14-x, \frac14-z$	47	y, x, z
24	$\frac14+y, \frac14+x, \frac14-z$	48	$\bar{y}, \bar{x}, z$

$+(0,\frac12,\frac12), (\frac12,0,\frac12), (\frac12,\frac12,0)$

Wyckoff Positions of Group 195 (*P*23)

Multiplicity	Wyckoff letter	Site symmetry	Coordinates
12	j	1	(x,y,z) (-x,-y,z) (-x,y,-z) (x,-y,-z) (z,x,y) (z,-x,-y) (-z,-x,y) (-z,x,-y) (y,z,x) (-y,z,-x) (y,-z,-x) (-y,-z,x)
6	i	2..	(x,1/2,1/2) (-x,1/2,1/2) (1/2,x,1/2) (1/2,-x,1/2) (1/2,1/2,x) (1/2,1/2,-x)
6	h	2..	(x,1/2,0) (-x,1/2,0) (0,x,1/2) (0,-x,1/2) (1/2,0,x) (1/2,0,-x)
6	g	2..	(x,0,1/2) (-x,0,1/2) (1/2,x,0) (1/2,-x,0) (0,1/2,x) (0,1/2,-x)
6	f	2..	(x,0,0) (-x,0,0) (0,x,0) (0,-x,0) (0,0,x) (0,0,-x)
4	e	.3.	(x,x,x) (-x,-x,x) (-x,x,-x) (x,-x,-x)
3	d	222 . .	(1/2,0,0) (0,1/2,0) (0,0,1/2)
3	c	222 . .	(0,1/2,1/2) (1/2,0,1/2) (1/2,1/2,0)
1	b	23.	(1/2,1/2,1/2)
1	a	23.	(0,0,0)

Wyckoff Positions of Group 227 (*Fd-3m*) [origin choice 1]

Multiplicity	Wyckoff letter	Site symmetry	Coordinates
			(0,0,0) + (0,1/2,1/2) + (1/2,0,1/2) + (1/2,1/2,0) +
192	i	1	(x,y,z) (-x,-y+1/2,z+1/2) (-x+1/2,y+1/2,-z) (x+1/2,-y,-z+1/2) (z,x,y) (z+1/2,-x,-y+1/2) (-z,-x+1/2,y+1/2) (-z+1/2,x+1/2,-y) (y,z,x) (-y+1/2,z+1/2,-x) (y+1/2,-z,-x+1/2) (-y,-z+1/2,x+1/2) (y+3/4,x+1/4,-z+3/4) (-y+1/4,-x+1/4,-z+1/4) (y+1/4,-x+3/4,z+3/4) (-y+3/4,x+3/4,z+1/4) (x+3/4,z+1/4,-y+3/4) (-x+3/4,z+3/4,y+1/4) (-x+1/4,-z+1/4,-y+1/4) (x+1/4,-z+3/4,y+3/4) (z+3/4,y+1/4,-x+3/4) (z+1/4,-y+3/4,x+3/4) (-z+3/4,y+3/4,x+1/4) (-z+1/4,-y+1/4,-x+1/4) (-x+1/4,-y+1/4,-z+1/4) (x+1/4,y+3/4,-z+3/4) (x+3/4,-y+3/4,z+1/4) (-x+3/4,y+1/4,z+3/4) (-z+1/4,-x+1/4,-y+1/4) (-z+3/4,x+1/4,y+3/4) (z+1/4,x+3/4,-y+3/4) (z+3/4,-x+3/4,y+1/4) (-y+1/4,-z+1/4,-x+1/4) (y+3/4,-z+3/4,x+1/4) (-y+3/4,z+1/4,x+3/4) (y+1/4,z+3/4,-x+3/4) (-y+1/2,-x,z+1/2) (y,x,z) (-y,x+1/2,-z+1/2) (y+1/2,-x+1/2,-z) (-x+1/2,-z,y+1/2) (x+1/2,-z+1/2,-y) (x,z,y) (-x,z+1/2,-y+1/2) (-z+1/2,-y,x+1/2) (-z,y+1/2,-x+1/2) (z+1/2,-y+1/2,-x) (z,y,x)
96	h	..2	(1/8,y,-y+1/4) (7/8,-y+1/2,-y+3/4) (3/8,y+1/2,y+3/4) (5/8,-y,y+1/4) (-y+1/4,1/8,y) (-y+3/4,7/8,-y+1/2) (y+3/4,3/8,y+1/2) (y+1/4,5/8,-y) (y,-y+1/4,1/8) (-y+1/2,-y+3/4,7/8) (y+1/2,y+3/4,3/8) (-y,y+1/4,5/8) (1/8,-y+1/4,y) (3/8,y+3/4,y+1/2) (7/8,-y+3/4,-y+1/2) (5/8,y+1/4,-y) (y,1/8,-y+1/4) (y+1/2,3/8,y+3/4) (-y+1/2,7/8,-y+3/4) (-y,5/8,y+1/4) (-y+1/4,y,1/8) (y+3/4,y+1/2,3/8) (-y+3/4,-y+1/2,7/8) (y+1/4,-y,5/8)
96	g	..m	(x,x,z) (-x,-x+1/2,z+1/2) (-x+1/2,x+1/2,-z) (x+1/2,-x,-z+1/2) (z,x,x) (z+1/2,-x,-x+1/2) (-z,-x+1/2,x+1/2) (-z+1/2,x+1/2,-x) (x,z,x) (-x+1/2,z+1/2,-x) (x+1/2,-z,-x+1/2) (-x,-z+1/2,x+1/2) (x+3/4,x+1/4,-z+3/4) (-x+1/4,-x+1/4,-z+1/4) (x+1/4,-x+3/4,z+3/4) (-x+3/4,x+3/4,z+1/4) (x+3/4,z+1/4,-x+3/4) (-x+3/4,z+3/4,x+1/4) (-x+1/4,-z+1/4,-x+1/4) (x+1/4,-z+3/4,x+3/4) (z+3/4,x+1/4,-x+3/4) (z+1/4,-x+3/4,x+3/4) (-z+3/4,x+3/4,x+1/4) (-z+1/4,-x+1/4,-x+1/4)
48	f	2.m m	(x,0,0) (-x,1/2,1/2) (0,x,0) (1/2,-x,1/2) (0,0,x) (1/2,1/2,-x) (3/4,x+1/4,3/4) (1/4,-x+1/4,1/4) (x+3/4,1/4,3/4) (-x+3/4,3/4,1/4) (3/4,1/4,-x+3/4) (1/4,3/4,x+3/4)
32	e	.3m	(x,x,x) (-x,-x+1/2,x+1/2) (-x+1/2,x+1/2,-x) (x+1/2,-x,-x+1/2) (x+3/4,x+1/4,-x+3/4) (-x+1/4,-x+1/4,-x+1/4) (x+1/4,-x+3/4,x+3/4) (-x+3/4,x+3/4,x+1/4)
16	d	.-3m	(5/8,5/8,5/8) (3/8,7/8,1/8) (7/8,1/8,3/8) (1/8,3/8,7/8)
16	c	.-3m	(1/8,1/8,1/8) (7/8,3/8,5/8) (3/8,5/8,7/8) (5/8,7/8,3/8)
8	b	-43m	(1/2,1/2,1/2) (1/4,3/4,1/4)
8	a	-43m	(0,0,0) (3/4,1/4,3/4)

Diffraction from a Truncated Surface

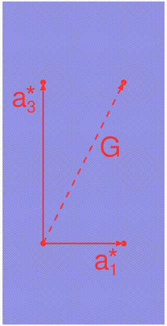

For an infinite sample, the diffraction spots are infinitesimally sharp.

Diffraction from a Truncated Surface

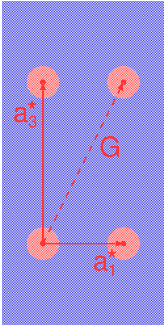

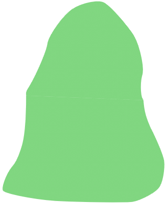

For an infinite sample, the diffraction spots are infinitesimally sharp.

With finite sample size, these spots grow in extent and become more diffuse.

Diffraction from a Truncated Surface

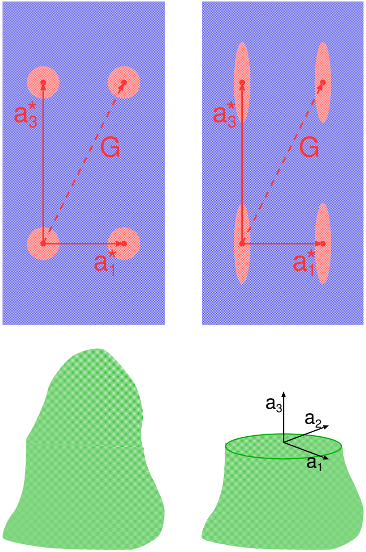

For an infinite sample, the diffraction spots are infinitesimally sharp.

With finite sample size, these spots grow in extent and become more diffuse.

If the sample is cleaved and left with flat surface, the diffraction will spread into rods perpendicular to the surface.

Diffraction from a Truncated Surface

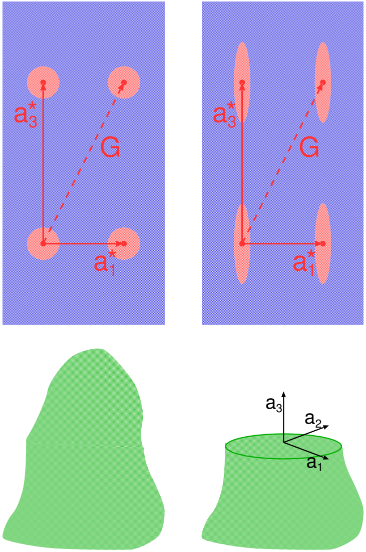

For an infinite sample, the diffraction spots are infinitesimally sharp.

With finite sample size, these spots grow in extent and become more diffuse.

If the sample is cleaved and left with flat surface, the diffraction will spread into rods perpendicular to the surface.

The scattering intensity can be obtained by treating the charge distribution as a convolution of an infinite sample with a step function in the z-direction.

CTR Scattering Factor

The scattering amplitude F^{CTR} along a crystal truncation rod is given by summing an infinite stack of atomic layers, each with scattering amplitude $A(\vec{Q})$.

CTR Scattering Factor

The scattering amplitude F^{CTR} along a crystal truncation rod is given by summing an infinite stack of atomic layers, each with scattering amplitude $A(\vec{Q})$.

$$F^{CTR} = A(\vec{Q}) \sum_{j=0}^{\infty} e^{iQ_z a_3 j}$$

CTR Scattering Factor

The scattering amplitude F^{CTR} along a crystal truncation rod is given by summing an infinite stack of atomic layers, each with scattering amplitude $A(\vec{Q})$.

$$F^{CTR} = A(\vec{Q}) \sum_{j=0}^{\infty} e^{iQ_z a_3 j}$$

this sum has been discussed previously and gives

CTR Scattering Factor

The scattering amplitude F^{CTR} along a crystal truncation rod is given by summing an infinite stack of atomic layers, each with scattering amplitude $A(\vec{Q})$.

$$F^{CTR} = A(\vec{Q}) \sum_{j=0}^{\infty} e^{iQ_z a_3 j}$$

$$= \frac{A(\vec{Q})}{1 - e^{iQ_z a_3}}$$

this sum has been discussed previously and gives

CTR Scattering Factor

The scattering amplitude F^{CTR} along a crystal truncation rod is given by summing an infinite stack of atomic layers, each with scattering amplitude $A(\vec{Q})$.

$$F^{CTR} = A(\vec{Q}) \sum_{j=0}^{\infty} e^{iQ_z a_3 j}$$

$$= \frac{A(\vec{Q})}{1 - e^{iQ_z a_3}} = \frac{A(\vec{Q})}{1 - e^{i2\pi l}}$$

this sum has been discussed previously and gives

or, in terms of the momentum transfer along the z-axis: $Q_z = 2\pi l/a_3$

CTR Scattering Factor

The scattering amplitude F^{CTR} along a crystal truncation rod is given by summing an infinite stack of atomic layers, each with scattering amplitude $A(\vec{Q})$.

$$F^{CTR} = A(\vec{Q}) \sum_{j=0}^{\infty} e^{iQ_z a_3 j}$$

this sum has been discussed previously and gives

$$= \frac{A(\vec{Q})}{1 - e^{iQ_z a_3}} = \frac{A(\vec{Q})}{1 - e^{i2\pi l}}$$

or, in terms of the momentum transfer along the z-axis: $Q_z = 2\pi l / a_3$

since the intensity is the square of the scattering factor

CTR Scattering Factor

The scattering amplitude F^{CTR} along a crystal truncation rod is given by summing an infinite stack of atomic layers, each with scattering amplitude $A(\vec{Q})$.

$$F^{CTR} = A(\vec{Q}) \sum_{j=0}^{\infty} e^{iQ_z a_3 j}$$

$$= \frac{A(\vec{Q})}{1 - e^{iQ_z a_3}} = \frac{A(\vec{Q})}{1 - e^{i2\pi l}}$$

this sum has been discussed previously and gives

or, in terms of the momentum transfer along the z-axis: $Q_z = 2\pi l / a_3$

since the intensity is the square of the scattering factor

$$I^{CTR} = \left| F^{CTR} \right|^2 = \frac{\left| A(\vec{Q}) \right|^2}{\left(1 - e^{i2\pi l}\right)\left(1 - e^{-i2\pi l}\right)}$$

CTR Scattering Factor

The scattering amplitude F^{CTR} along a crystal truncation rod is given by summing an infinite stack of atomic layers, each with scattering amplitude $A(\vec{Q})$.

$$F^{CTR} = A(\vec{Q}) \sum_{j=0}^{\infty} e^{iQ_z a_3 j}$$

$$= \frac{A(\vec{Q})}{1 - e^{iQ_z a_3}} = \frac{A(\vec{Q})}{1 - e^{i2\pi l}}$$

this sum has been discussed previously and gives

or, in terms of the momentum transfer along the z-axis: $Q_z = 2\pi l / a_3$

since the intensity is the square of the scattering factor

$$I^{CTR} = \left| F^{CTR} \right|^2 = \frac{\left| A(\vec{Q}) \right|^2}{\left(1 - e^{i2\pi l}\right)\left(1 - e^{-i2\pi l}\right)} = \frac{\left| A(\vec{Q}) \right|^2}{4 \sin^2(\pi l)}$$

Dependence on Q

When l is an integer (meeting the Laue condition), the scattering factor is infinite but just off this value, the scattering factor can be computed by letting $Q_z = q_z + 2\pi/a_3$, with q_z small.

Dependence on Q

When l is an integer (meeting the Laue condition), the scattering factor is infinite but just off this value, the scattering factor can be computed by letting $Q_z = q_z + 2\pi/a_3$, with q_z small.

$$I^{CTR} = \frac{\left|A(\vec{Q})\right|^2}{4\sin^2\left(Q_z a_3/2\right)}$$

Dependence on Q

When l is an integer (meeting the Laue condition), the scattering factor is infinite but just off this value, the scattering factor can be computed by letting $Q_z = q_z + 2\pi/a_3$, with q_z small.

$$I^{CTR} = \frac{\left|A(\vec{Q})\right|^2}{4\sin^2\left(Q_z a_3/2\right)} = \frac{\left|A(\vec{Q})\right|^2}{4\sin^2\left(\pi l + q_z a_3/2\right)}$$

Dependence on Q

When l is an integer (meeting the Laue condition), the scattering factor is infinite but just off this value, the scattering factor can be computed by letting $Q_z = q_z + 2\pi/a_3$, with q_z small.

$$I^{CTR} = \frac{\left|A(\vec{Q})\right|^2}{4\sin^2(Q_z a_3/2)} = \frac{\left|A(\vec{Q})\right|^2}{4\sin^2(\pi l + q_z a_3/2)}$$

$$= \frac{\left|A(\vec{Q})\right|^2}{4\sin^2(q_z a_3/2)}$$

Dependence on Q

When l is an integer (meeting the Laue condition), the scattering factor is infinite but just off this value, the scattering factor can be computed by letting $Q_z = q_z + 2\pi/a_3$, with q_z small.

$$I^{CTR} = \frac{\left|A(\vec{Q})\right|^2}{4\sin^2\left(Q_z a_3/2\right)} = \frac{\left|A(\vec{Q})\right|^2}{4\sin^2\left(\pi l + q_z a_3/2\right)}$$

$$= \frac{\left|A(\vec{Q})\right|^2}{4\sin^2\left(q_z a_3/2\right)} \approx \frac{\left|A(\vec{Q})\right|^2}{4(q_z a_3/2)^2}$$

Dependence on Q

When l is an integer (meeting the Laue condition), the scattering factor is infinite but just off this value, the scattering factor can be computed by letting $Q_z = q_z + 2\pi/a_3$, with q_z small.

$$I^{CTR} = \frac{\left|A(\vec{Q})\right|^2}{4\sin^2\left(Q_z a_3/2\right)} = \frac{\left|A(\vec{Q})\right|^2}{4\sin^2\left(\pi l + q_z a_3/2\right)}$$

$$= \frac{\left|A(\vec{Q})\right|^2}{4\sin^2\left(q_z a_3/2\right)} \approx \frac{\left|A(\vec{Q})\right|^2}{4(q_z a_3/2)^2} = \frac{\left|A(\vec{Q})\right|^2}{q_z^2 a_3^2}$$

Dependence on Q

When l is an integer (meeting the Laue condition), the scattering factor is infinite but just off this value, the scattering factor can be computed by letting $Q_z = q_z + 2\pi/a_3$, with q_z small.

$$I^{CTR} = \frac{\left|A(\vec{Q})\right|^2}{4\sin^2(Q_z a_3/2)} = \frac{\left|A(\vec{Q})\right|^2}{4\sin^2(\pi l + q_z a_3/2)}$$

$$= \frac{\left|A(\vec{Q})\right|^2}{4\sin^2(q_z a_3/2)} \approx \frac{\left|A(\vec{Q})\right|^2}{4(q_z a_3/2)^2} = \frac{\left|A(\vec{Q})\right|^2}{q_z^2 a_3^2}$$

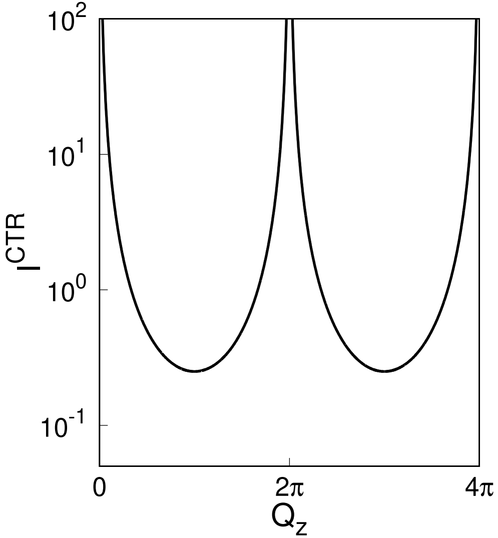

Absorption Effect

Absorption effects can be included as well by adding a term for each layer penetrated

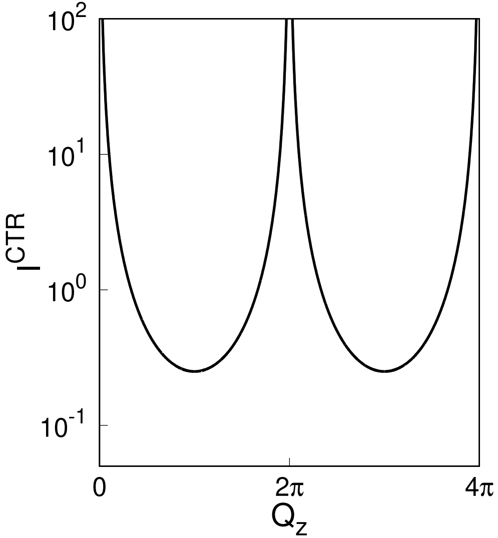

Absorption Effect

Absorption effects can be included as well by adding a term for each layer penetrated

$$F^{CTR} = A(\vec{Q}) \sum_{j=0}^{\infty} e^{iQ_z a_3 j}$$

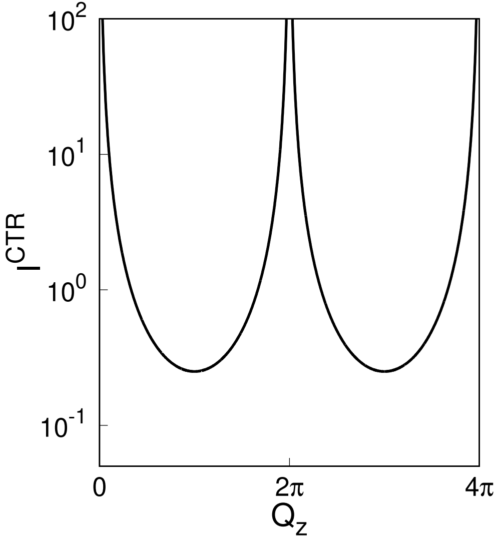

Absorption Effect

Absorption effects can be included as well by adding a term for each layer penetrated

$$F^{CTR} = A(\vec{Q}) \sum_{j=0}^{\infty} e^{iQ_z a_3 j} e^{-\beta j}$$

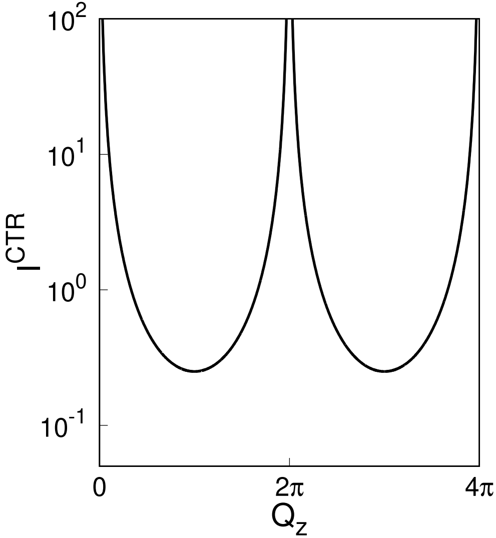

Absorption Effect

Absorption effects can be included as well by adding a term for each layer penetrated

$$F^{CTR} = A(\vec{Q}) \sum_{j=0}^{\infty} e^{iQ_z a_3 j} e^{-\beta j}$$
$$= \frac{A(\vec{Q})}{1 - e^{iQ_z a_3} e^{-\beta}}$$

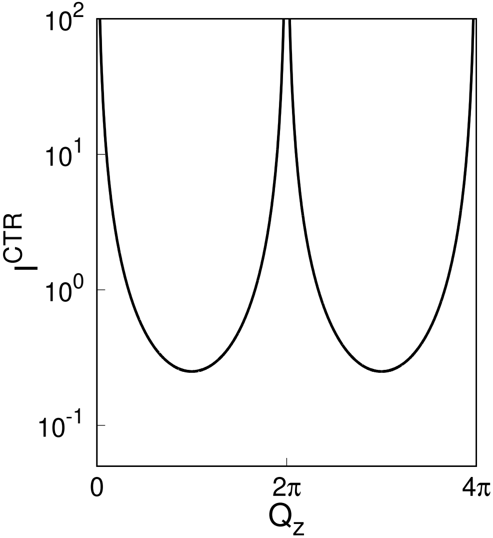

Absorption Effect

Absorption effects can be included as well by adding a term for each layer penetrated

$$F^{CTR} = A(\vec{Q}) \sum_{j=0}^{\infty} e^{iQ_z a_3 j} e^{-\beta j}$$

$$= \frac{A(\vec{Q})}{1 - e^{iQ_z a_3} e^{-\beta}}$$

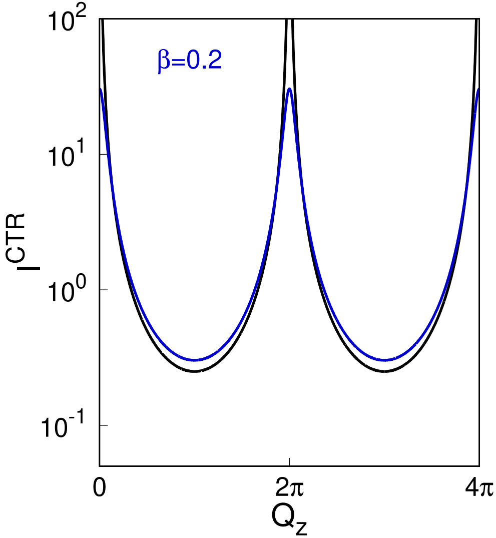

Absorption Effect

Absorption effects can be included as well by adding a term for each layer penetrated

$$F^{CTR} = A(\vec{Q}) \sum_{j=0}^{\infty} e^{iQ_z a_3 j} e^{-\beta j}$$

$$= \frac{A(\vec{Q})}{1 - e^{iQ_z a_3} e^{-\beta}}$$

This removes the infinity and increases the scattering profile of the crystal truncation rod

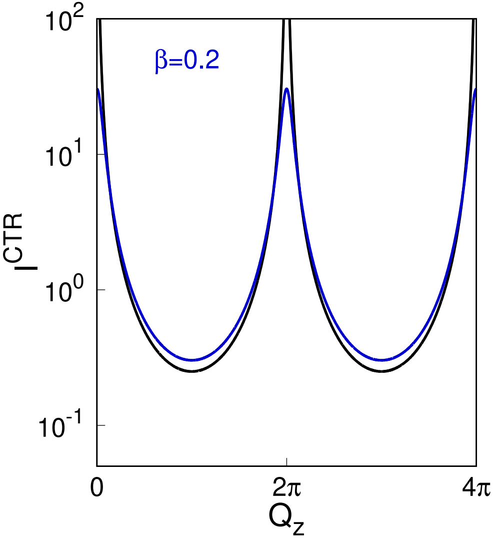

Density Effect

The CTR profile is sensitive to the termination of the surface. This makes it an ideal probe of electron density of adsorbed species or single atom overlayers.

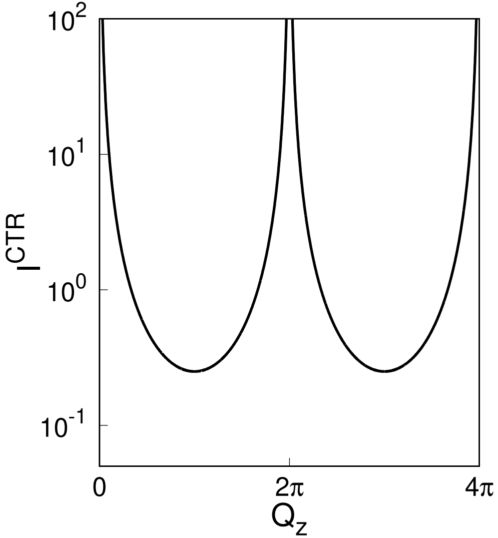

Density Effect

The CTR profile is sensitive to the termination of the surface. This makes it an ideal probe of electron density of adsorbed species or single atom overlayers.

$$F^{total} = F^{CTR} + F^{top\ layer}$$

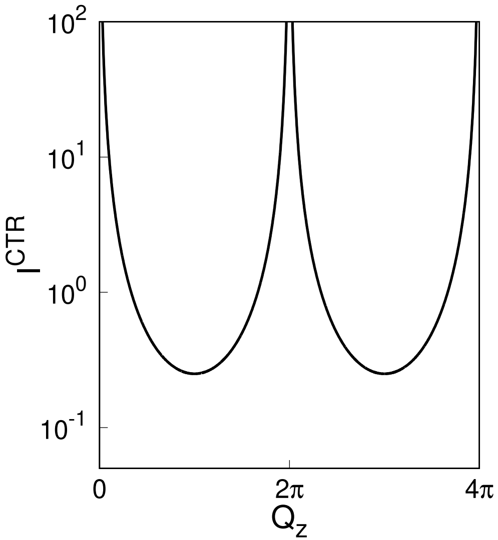

Density Effect

The CTR profile is sensitive to the termination of the surface. This makes it an ideal probe of electron density of adsorbed species or single atom overlayers.

$$F^{total} = F^{CTR} + F^{top\ layer}$$
$$= \frac{A(\vec{Q})}{1 - e^{i2\pi l}}$$

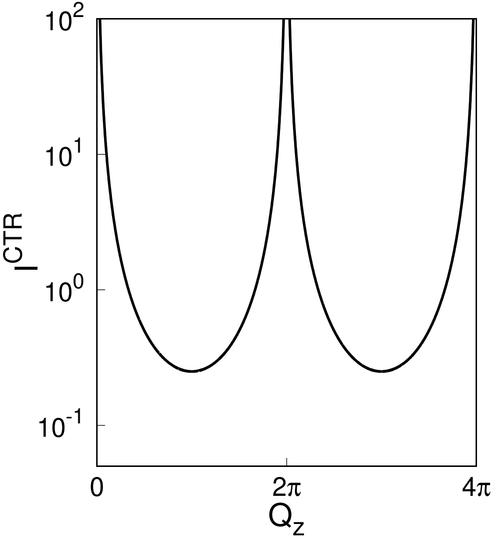

Density Effect

The CTR profile is sensitive to the termination of the surface. This makes it an ideal probe of electron density of adsorbed species or single atom overlayers.

$$F^{total} = F^{CTR} + F^{top\ layer}$$

$$= \frac{A(\vec{Q})}{1 - e^{i2\pi l}} + A(\vec{Q})e^{-i2\pi(1+z_0)l}$$

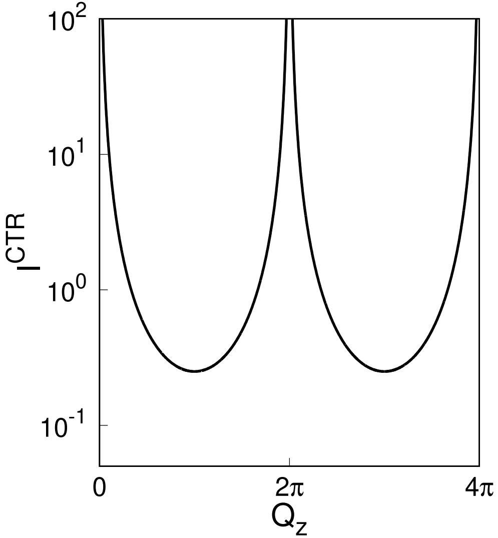

Density Effect

The CTR profile is sensitive to the termination of the surface. This makes it an ideal probe of electron density of adsorbed species or single atom overlayers.

$$F^{total} = F^{CTR} + F^{top\ layer}$$
$$= \frac{A(\vec{Q})}{1 - e^{i2\pi l}} + A(\vec{Q})e^{-i2\pi(1+z_0)l}$$

where z_0 is the relative displacement of the top layer from the bulk lattice spacing a_3

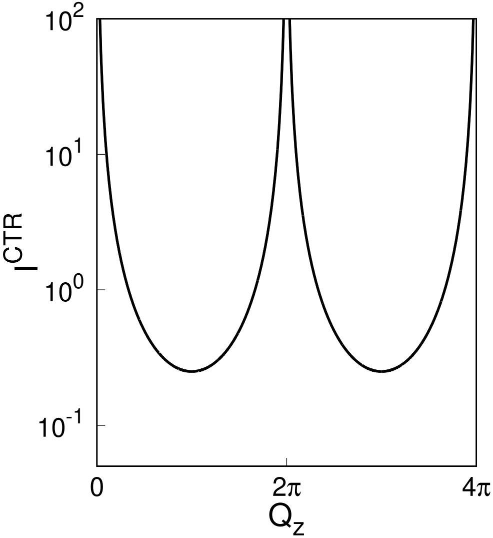

Density Effect

The CTR profile is sensitive to the termination of the surface. This makes it an ideal probe of electron density of adsorbed species or single atom overlayers.

$$F^{total} = F^{CTR} + F^{top\ layer}$$
$$= \frac{A(\vec{Q})}{1 - e^{i2\pi l}} + A(\vec{Q})e^{-i2\pi(1+z_0)l}$$

where z_0 is the relative displacement of the top layer from the bulk lattice spacing a_3

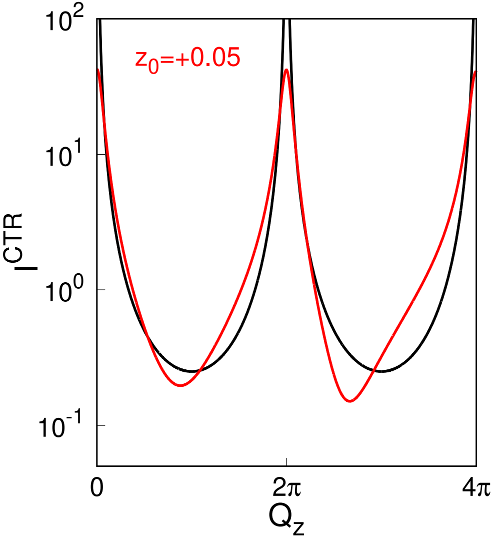

Density Effect

The CTR profile is sensitive to the termination of the surface. This makes it an ideal probe of electron density of adsorbed species or single atom overlayers.

$$F^{total} = F^{CTR} + F^{top\ layer}$$
$$= \frac{A(\vec{Q})}{1 - e^{i2\pi l}} + A(\vec{Q})e^{-i2\pi(1+z_0)l}$$

where z_0 is the relative displacement of the top layer from the bulk lattice spacing a_3

This effect gets larger for larger momentum transfers

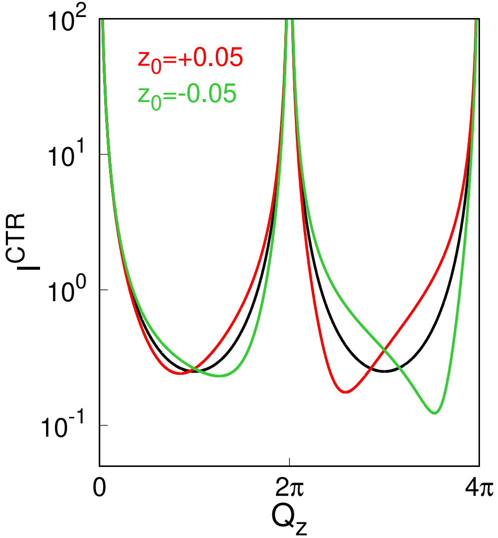

Density Effect

The CTR profile is sensitive to the termination of the surface. This makes it an ideal probe of electron density of adsorbed species or single atom overlayers.

$$F^{total} = F^{CTR} + F^{top\ layer}$$
$$= \frac{A(\vec{Q})}{1 - e^{i2\pi l}} + A(\vec{Q}) e^{-i2\pi(1+z_0)l}$$

where z_0 is the relative displacement of the top layer from the bulk lattice spacing a_3

This effect gets larger for larger momentum transfers

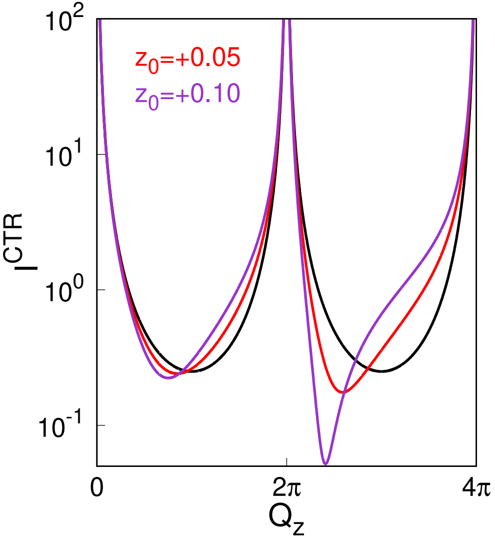

Hydrated surface of magnetite

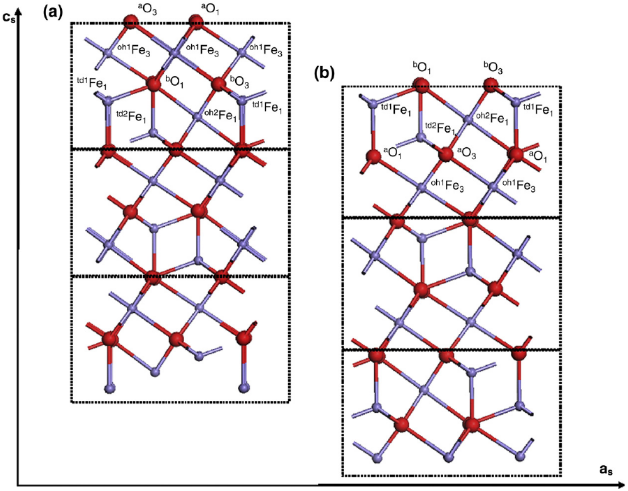

"Surface structure of magnetite (111) under hydrated conditions by crystal truncation rod diffraction," S.C. Petitto et al. *Surf. Sci.* **604**, 1082-1093 (2010).

Hydrated surface of magnetite

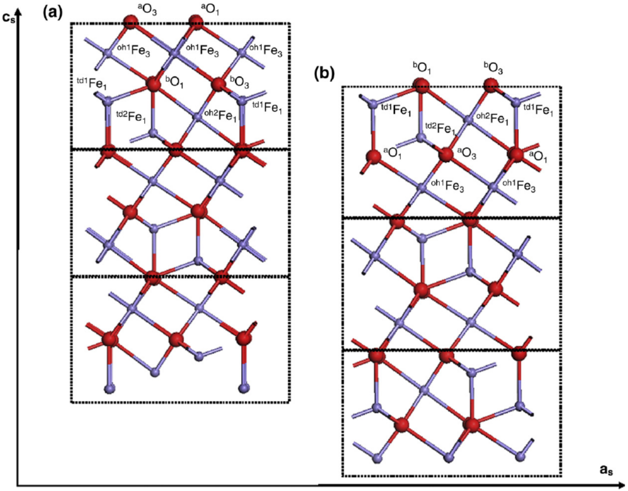

Magnetite, Fe_3O_4, is a technologically important material for environmental remediation

"Surface structure of magnetite (111) under hydrated conditions by crystal truncation rod diffraction," S.C. Petitto et al. *Surf. Sci.* **604**, 1082-1093 (2010).

Hydrated surface of magnetite

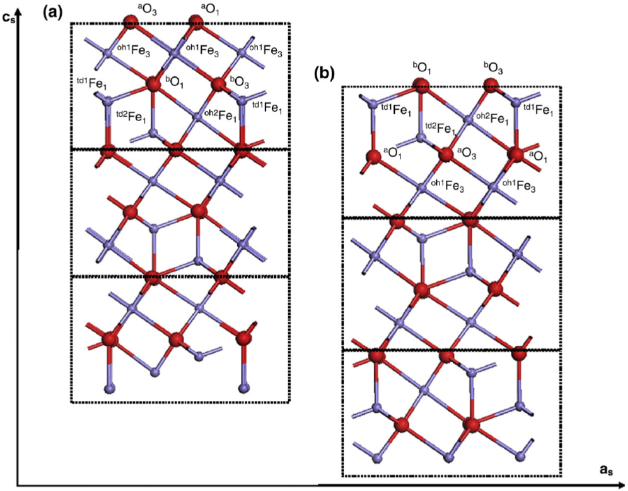

Magnetite, Fe_3O_4, is a technologically important material for environmental remediation

It is important to know the structure of the surface of magnetite in a hydrated environment to understand the processes that favor sorption of heavy elements

"Surface structure of magnetite (111) under hydrated conditions by crystal truncation rod diffraction," S.C. Petitto et al. *Surf. Sci.* **604**, 1082-1093 (2010).

Hydrated surface of magnetite

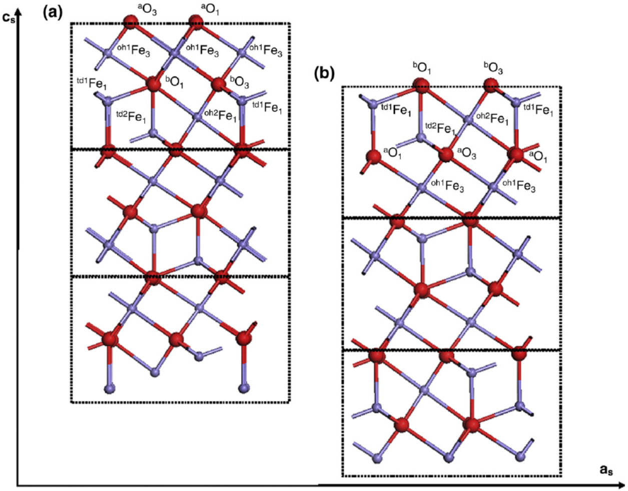

Magnetite, Fe_3O_4, is a technologically important material for environmental remediation

It is important to know the structure of the surface of magnetite in a hydrated environment to understand the processes that favor sorption of heavy elements

There are two possible surfaces, the oxygen octahedral iron, OOI (a), and the oxygen mixed-iron, OMI (b), terminations

"Surface structure of magnetite (111) under hydrated conditions by crystal truncation rod diffraction," S.C. Petitto et al. *Surf. Sci.* **604**, 1082-1093 (2010).

Magnetite (111) surface

Crystal truncation rod measurements require an oriented single crystal with a polished and cleaned surface.

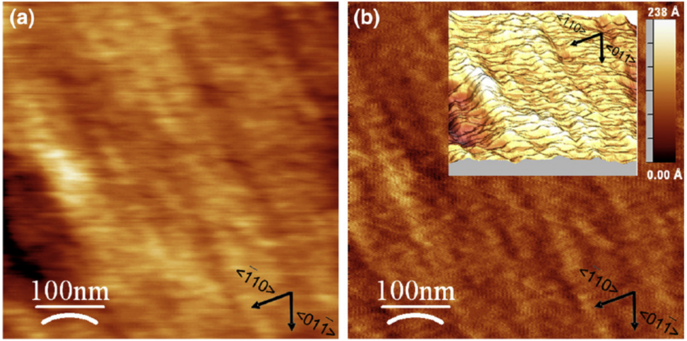

"Surface structure of magnetite (111) under hydrated conditions by crystal truncation rod diffraction," S.C. Petitto et al. *Surf. Sci.* **604**, 1082-1093 (2010).

Magnetite (111) surface

Crystal truncation rod measurements require an oriented single crystal with a polished and cleaned surface.

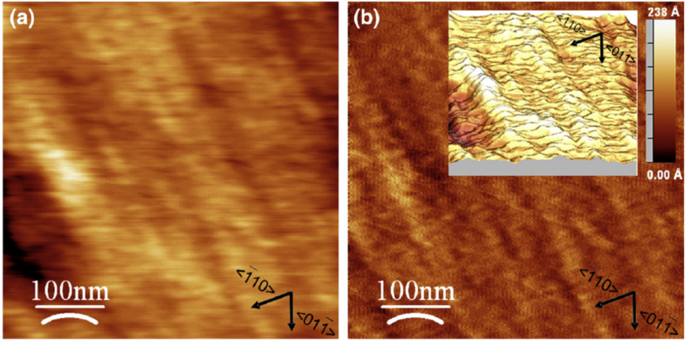

The final polished surface has clear terraces of between 150 Å–700 Å and a surface roughness of about 1.4 Å as seen in the inset from the atomic force microscopy images

"Surface structure of magnetite (111) under hydrated conditions by crystal truncation rod diffraction," S.C. Petitto et al. *Surf. Sci.* **604**, 1082-1093 (2010).

CTR data and modeling

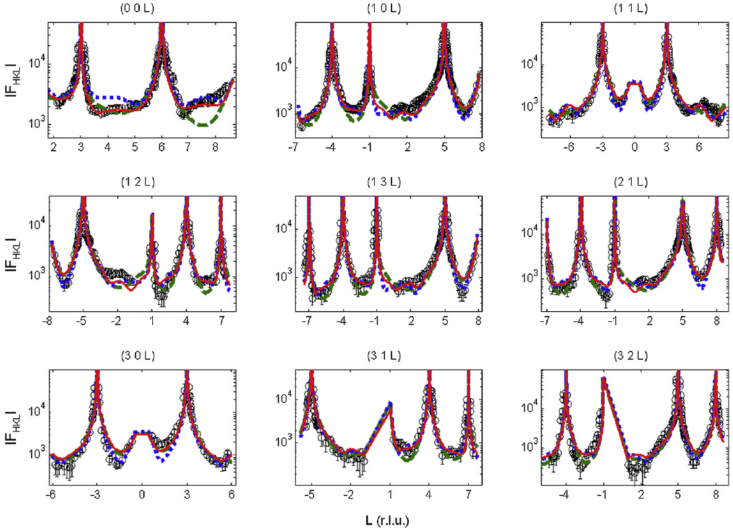

"Surface structure of magnetite (111) under hydrated conditions by crystal truncation rod diffraction," S.C. Petitto et al. *Surf. Sci.* **604**, 1082-1093 (2010).

Hydrated surface of magnetite

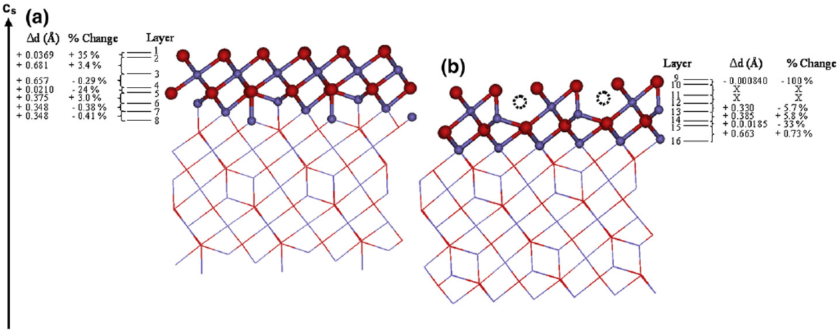

"Surface structure of magnetite (111) under hydrated conditions by crystal truncation rod diffraction," S.C. Petitto et al. *Surf. Sci.* **604**, 1082-1093 (2010).

Hydrated surface of magnetite

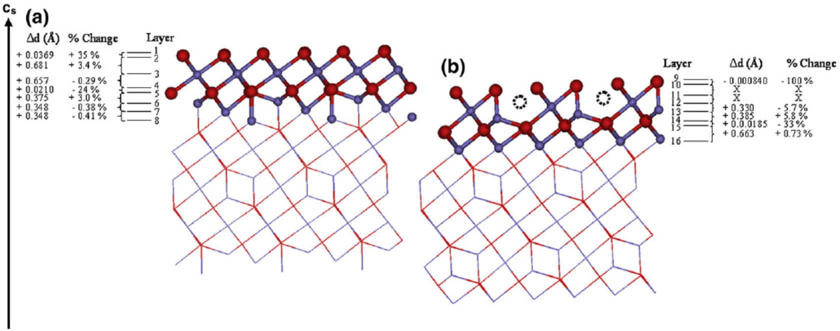

The result of the modeling of the CTR data indicates that the surface is 75% OOI and 25% OMI

"Surface structure of magnetite (111) under hydrated conditions by crystal truncation rod diffraction," S.C. Petitto et al. *Surf. Sci.* **604**, 1082-1093 (2010).

Hydrated surface of magnetite

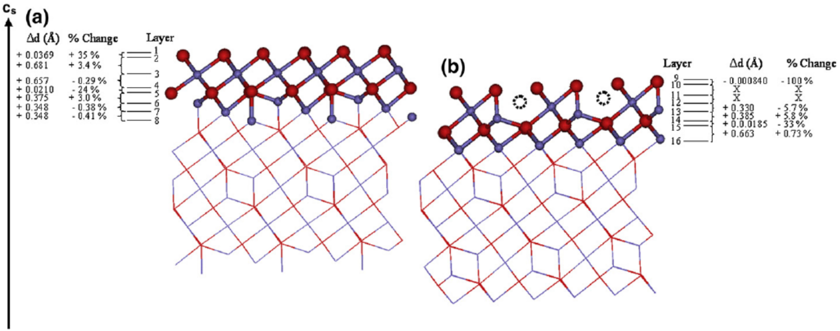

The result of the modeling of the CTR data indicates that the surface is 75% OOI and 25% OMI

The modeling also can provide details about the distance changes in the first layers at the surface

"Surface structure of magnetite (111) under hydrated conditions by crystal truncation rod diffraction," S.C. Petitto et al. *Surf. Sci.* **604**, 1082-1093 (2010).